ChemComm

COMMUNICATION

View Article Online
View Journal | View Issue

Cite this: *Chem. Commun.*, 2015, 51, 5326

Received 31st October 2014,
Accepted 31st December 2014

DOI: 10.1039/c4cc08613a

www.rsc.org/chemcomm

Determination of receptor specificities for whole influenza viruses using multivalent glycan arrays†

Mia L. Huang,[a] Miriam Cohen,[b] Christopher J. Fisher,[a] Robert T. Schooley,[c] Pascal Gagneux[b] and Kamil Godula*[a]

Influenza viruses bind to mucosal glycans to gain entry into a host organism and initiate infection. The target glycans are often displayed in multivalent arrangements on proteins; however, how glycan presentation influences viral specificity is poorly understood. Here, we report a microarray platform approximating native glycan display to facilitate such studies.

Pathogens rely on molecular recognition events at the cell surface to gain entry into a host organism.[1] As such, many pathogens have evolved to exploit glycans that are abundantly distributed on target epithelial tissues to initiate infection.[2] Influenza A virus (IAV) offers a prime example of this evolutionary adaptation. Its virion displays trimeric hemagglutinin (HA) proteins that bind to sialoside glycans presented on host glycoproteins, called mucins, to facilitate virion internalization. IAV also maintains tetrameric neuraminidase (NA) enzymes that cleave sialic acids to allow detachment from the cell surface. NA, a receptor-destroying enzyme, works in careful balance with HA proteins to enable newly produced viruses to leave infected cells and propagate infection. Another likely role for NA is to free bound virus from secreted host mucins, which can present glycans similar to those on the underlying tissue and serve as protective decoys covering mucosal epithelia and sequestering viruses to prevent infection.[3]

While terminal sialic acid is a carbohydrate residue universally recognized by all influenza strains, the nature of its attachment to the underlying glycan structures of glycoproteins determines viral specificity for distinct host species.[4] In the human upper airway, such glycans display sialic acid residues linked predominantly *via* α2-6 glycosidic linkages, while the lower respiratory tract and the secreted mucin decoys are rich in α2-3 sialoglycans.[5] In contrast, most influenza viruses populating both wild and domesticated birds show preference for α2-3 linked sialic acids, which is prevalent in avian gastrointestinal epithelia.[6] Mutations in the viral HA binding site that switch selectivity from α2-3 to α2-6 sialoglycans is a prerequisite for interspecies transfer and can be indicative of a newly acquired ability of avian viruses to infect humans.[7–9] As such, screening tools to identify changes in influenza glycan specificity have been utilized for early indication of virus transmissibility and assessment of potential pandemic risks.

While individual sialoglycan structures are important determinants of influenza binding, the spatial presentation of these glycans may play a major role in the determination of IAV receptor specificity. The virus relies on avidity effects to compensate for the weak affinity and low selectivity of HA binding to individual sialoglycan structures ($K_d \sim 2$ mM).[10] Mucosal barriers are composed primarily of mucins, which are large protein scaffolds densely decorated with sialoglycans (Fig. 1).[11] The multivalency of glycan display in mucins is matched by the high density of HA on the surface of influenza virions

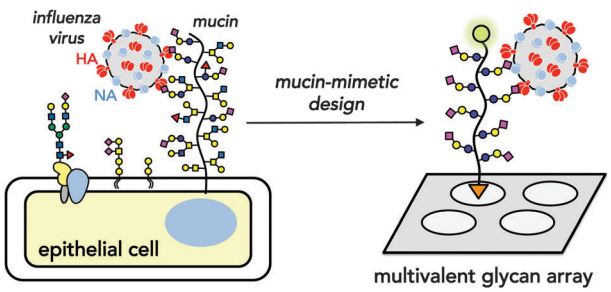

Fig. 1 Influenza A viruses engage sialoside glycans arranged on epithelial mucins to initiate infection. A mucin-mimetic microarray platform can serve as a tool to investigate how parameters such as glycan structure, valency and surface density influence binding and specificity of the pathogen.

[a] *Department of Chemistry and Biochemistry, University of California San Diego, 9500 Gilman Drive, San Diego, CA, 92093-0358, USA. E-mail: kgodula@ucsd.edu*
[b] *Department of Pathology, Division of Comparative Pathology and medicine, University of California San Diego, 9500 Gilman Drive, San Diego, CA, 92093-0687, USA*
[c] *Division of Infectious Diseases, Department of Medicine, University of California San Diego, 9500 Gilman Drive, San Diego, CA, 92093-0358, USA*

† Electronic supplementary information (ESI) available: Materials and methods, analytical data, and copies of NMR spectra for compounds **1**, **2a–c**, and other synthetic intermediates. See DOI: 10.1039/c4cc08613a

(~200–1000 copies of HA trimers per virus),[12,13] resulting in specific high-avidity binding of the virus to the mucosal membranes. It is known that increasing the surface density of glycans can result in altered selectivity of lectins for their glycan ligands;[14,15] however, the parameters that define how multivalency affects viral binding and specificity have not yet been fully established. High-throughput screening platforms will be needed to systematically interrogate the binding of whole viruses to sialoglycans presented in a manner that resembles their organization in mucosal barriers.

Glycan microarrays have emerged as a powerful tool for determining the ligand specificities of glycan-binding proteins (GBPs).[16–18] In a traditional format, individual glycan structures are immobilized on the array surface to create a multivalent ligand display that can elicit sufficiently strong binding by GBPs. This technology has enabled important studies that provided key insights into the glycan specificity of HAs derived from influenza strains involved in recent pandemics;[19] yet, surprisingly few studies have been reported using these platforms to obtain information about the binding of intact viruses.[20–23] One limitation of the current glycan array technology is the lack of control over glycan presentation. This is compounded by the difficulties associated with the characterization of the arrays, including the determination of parameters such as surface density and spatial distribution of glycans after immobilization. Recent studies comparing different glycan array platforms have revealed that distinct glycan grafting strategies could influence their recognition by GBPs.[24] Perhaps more importantly, the two-dimensional glycan display in the current microarray format is limited in its ability to recapitulate the three-dimensional glycan presentation on cell surface glycoproteins, thus, obscuring higher-order binding events (and their physiological consequences) between the multivalent glycoconjugates and their oligomeric receptors, such as the influenza virion.

To address this limitation, a new generation of glycan microarrays have begun to emerge, where individual glycan structures are displayed on synthetic multivalent scaffolds that approximate the presentation of glycans in native glycoproteins.[25] These platforms that use synthetic neo-glycoproteins,[26] glycodendrimers,[27] or glycopolymers[28] as mimetics of the various glycoconjugates found on the surfaces of cells are beginning to reveal the subtle effects of three-dimensional glycan presentation on their recognition by GBPs.[29,30] Inspired by this work and the rich history of linear glycopolymers as soluble probes for analysing influenza binding,[31–33] we have developed, and report here, a microarray that utilizes glycopolymers to create a presentation of sialoglycans resembling their native display on mucosal membranes and allows for the interrogation of glycan binding preferences of intact influenza viruses.

To create a microarray platform, which could potentially accommodate a large repertoire of glycan structures found in mucins, we designed a polymer scaffold that can be rapidly assembled into glycopolymers while circumventing the challenges associated with carbohydrate synthesis or pre-functionalization. We have previously reported an acrylamide polymer decorated with pendant *N*-methylaminooxy groups that is primed for direct attachment of unmodified glycans available from natural or commercial sources.[34] Such α-heteroatom nucleophiles are known to react with the reducing terminus of various glycans producing stable *N*-glycopyranosides.[35] Here we describe the use of this strategy to generate glycopolymers displaying sialoglycans that can be recognized by influenza.

Using the RAFT technique,[36] we first prepared polymer precursor **1** with well-defined lengths (DP ~ 200) and narrow chain length distributions (DI ~ 1.18), carrying reactive *N*-methylaminooxy side-chains.[34] The polymer was end-functionalized with an azide group for covalent conjugation on cyclooctyne-coated glass and a tetramethylrhodamine (TAMRA) fluorophore for quantification of the extent of glycopolymer immobilization to the microarray surface. Ligation of glycans to **1** (1.1 equiv. of glycan per reactive side-chain) proceeded smoothly under acidic conditions (1 M sodium acetate buffer, pH = 4.5) at 50 °C for 72 h, affording lactose (**2a**), 3′-sialyllactose (α2-3, **2b**), and 6′-sialyllactose (α2-6, **2c**) glycopolymers in high yields (see ESI†). The lower ligation efficiency observed for 3′- and 6′-sialyllactose (45%) compared to lactose (70%) is likely due to the larger size of these glycans and to charge repulsion due to the presence of carboxylate groups in the sialic acid residues (Fig. 2).

Printing of the resulting glycopolymers on cyclooctyne-coated slides[34] produced microarrays of increasing glycopolymer densities. Using a robotic spotter, glycopolymers **2a–c** dissolved in a printing buffer (0.005% Tween 20 in PBS) were dispensed at a range of increasing glycan concentrations (1 μM to 10 mM) and the resulting arrays were stored at 4 °C overnight to allow sufficient time for glycopolymer grafting *via* the strain-promoted azide–alkyne cycloaddition[37] to proceed. The slides were then washed (0.1% Triton X-100 in PBS) to remove excess unbound material and the immobilized TAMRA-labelled glycopolymers were imaged using a fluorescence scanner to obtain an image of the resulting glycopolymer microarray (Fig. 3A). A plot of fluorescence emission intensity at λ_{max} = 535 nm as a function of glycan concentration during printing (Fig. 3B) indicates that the density of glycopolymers on the microarray surface can be

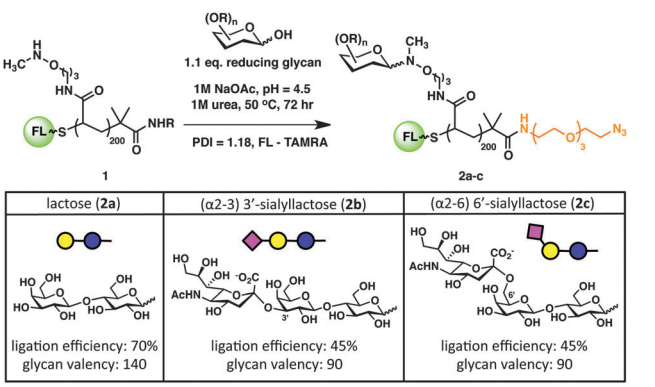

Fig. 2 Glycopolymer synthesis. Condensation of reactive polymer **1** with reducing glycans yielded fluorescent glycopolymers **2a–c** primed with an azido-group for immobilization on cyclooctyne-coated microarray substrates.

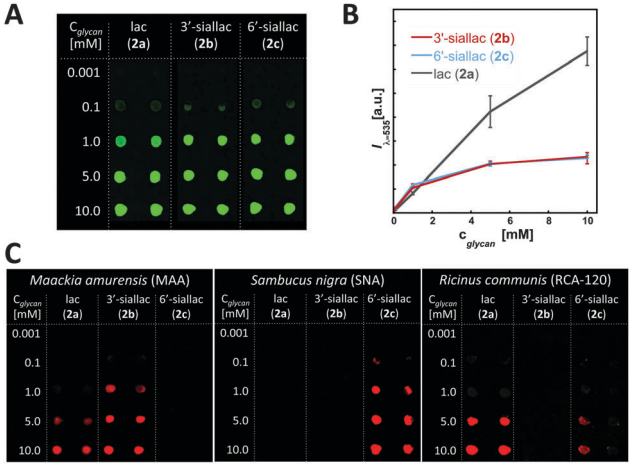

Fig. 3 Density variant glycan microarray was fabricated by printing TAMRA-labeled glycopolymers **2a–c** at increasing glycan concentrations (c_{glycan} = 1 μM to 10 mM) (A). The negatively charged sialoglycan polymers **2b** and **c** showed comparable surface grafting efficiency (B). The arrayed glycopolymers were recognized by lectins according to the structure of their pendant glycans (C).

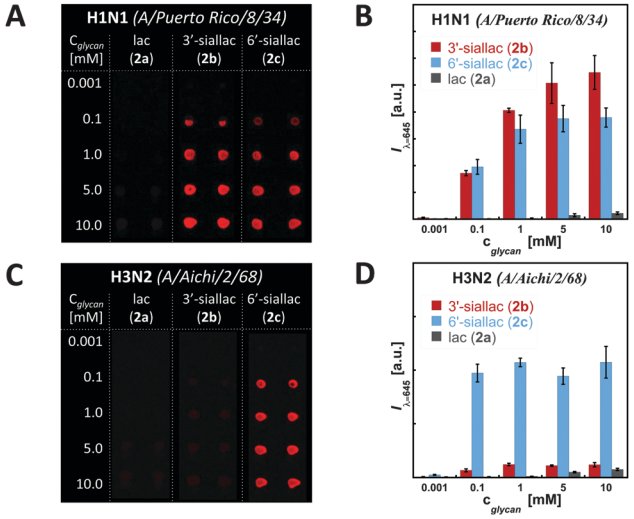

Fig. 4 Intact influenza A viruses were introduced to the microarray, visualized using immunostaining of their HA proteins, and analysed for specificity toward individual glycopolymers. While H1N1 (A/Puerto Rico/8/34) virus bound to both sialoglycan polymers (A), it exhibited a preference for 3′-sialyllactose epitopes (B). The H3N2 (A/Aichi/2/68) virus bound exclusively to the 6′-sialyllactose glycopolymers (C and D), consistent with its known specificity.

modulated and is a function of both the polymer concentration in the printing buffer as well as the structure of the pendant glycans. While the maximum surface density for 3′- and 6′-sialyllactose polymers was achieved at glycan concentrations of ~5 mM, the lactose glycopolymer did not reach surface saturation over the entire range of printing concentrations. This is not surprising, since the larger size and negative charge of the sialoglycans is expected to limit the accessibility and, thus, grafting efficiency of the glycopolymer chains to the substrate.

The resulting density variant glycan arrays were then evaluated for binding by a set of lectins with known glycan specificities. The slides were incubated for 1 h with *Maackia amurensis* agglutinin (MAA)[38] and *Sambucus nigra* agglutinin (SNA)[39] with preference for 3′- and 6′-sialoglycans, respectively, as well as *Ricinus communis* agglutinin (RCA-120)[20] that recognizes terminal galactose residues. Fig. 3C shows that the arrayed glycopolymers were recognized selectively by these lectins according to the structures of their pendant glycans (for experimental details see ESI†).

Once the selectivity of the surface-bound glycopolymers toward lectins was established, the arrays were tested for binding of influenza viruses. Whole H1N1 (A/Puerto Rico/8/34) and H3N2 (A/Aichi/2/68) viruses were incubated on the array for 1 h at ambient temperature. Thereafter, the slides were washed (PBS), fixed (2% paraformaldehyde in PBS, 30 min), and probed with anti-H1 (A/California/06/09) and anti-H3 (A/Shandong/9/99) antibodies for 30 min. Immunostaining with secondary antibodies appropriately labelled to emit fluorescence at λ_{max} = 645 nm was used to detect viruses that remained bound to the microarray surface.

We observed robust binding for both viruses according to their established glycan specificities (Fig. 4).[40,41] H1N1 (A/Puerto Rico/8/34) is known to engage both 3′- and 6′-sialoglycans and, accordingly, this virus bound to both sialoglycan polymers **2b** and **2c** in the microarray (Fig. 4A). In contrast, the H3N2 (A/Aichi/2/68) virus, which recognizes exclusively 6′-sialoglycans, engaged only the 6′-sialyllactose glycopolymer **2c** (Fig. 4C). Importantly, neither virus bound to the lactose glycopolymer **2a**, which lacks sialic acid residues, or the polymer backbone alone (for full microarray see ESI†).

Our glycan array platform reveals additional information about viral binding as a function of glycan presentation at the surface. The fluorescence tag in the arrayed polymers allows for determination of the relative glycan densities across the microarray, and thus, for direct comparison of viral binding to the various sialoglycan presentations. As expected, the amount of virus bound in the microarray generally increases with increasing glycopolymer density (Fig. 4B and D). Interestingly, while at lower surface densities, we did not observe significant preference of H1N1 binding for either glycoconjugate; the virus showed consistently enhanced binding to the more densely grafted 3′-sialyllactose polymers (Fig. 4B). While we have yet to fully investigate this phenomenon and its biological relevance in the context of viral specificity, our observations suggest the possible role of glycan presentation in modulating the specificity of the pathogen.

The mucin mimetic array offers a convenient and quantitative analytical platform to systematically evaluate various parameters, such as glycan structure, valency, and surface density, which define the interactions of viruses with their glycoprotein ligands. In addition, the ease and modularity of the glycopolymer assembly offers rapid access to multivalent mucin-like ligands with a broad diversity of glycan structures that can be integrated within the microarray platform. The ability to systematically evaluate viral interactions in the context of multivalency of glycan presentation on mucosal membranes and the oligomeric state of

viral glycan receptors may provide new insights into the mechanisms of the earliest stages of influenza entry as well as its infectivity and potential for interspecies transmission.

This work was supported by start-up funds from UCSD and the NIH Pathway to Independence Award (NIBIB: 5 R00 EB013446-04) to KG and by the G. Harold & Leila Y. Mathers Foundation to PG. CJF was supported in part by the UCSD Molecular Biophysics Training Program through the National Institute of Health (NIGMS: T32 GM08326).

Notes and references

1 A. Imberty and A. Varrot, *Curr. Opin. Struct. Biol.*, 2008, **18**, 567–576.
2 J. R. Bishop and P. Gagneux, *Glycobiology*, 2007, **17**, 23R–34R.
3 M. Cohen, X.-Q. Zhang, H. P. Senaati, H.-W. Chen, N. M. Varki, R. T. Schooley and P. Gagneux, *Virol. J.*, 2013, **10**, 321–323.
4 Y. Suzuki, T. Ito, T. Suzuki, R. E. J. Holland, T. M. Chambers, M. Kiso, H. Ishida and Y. Kawaoka, *J. Virol.*, 2000, **74**, 11825–11831.
5 P. Gagneux, M. Cheriyan, N. Hurtado-Ziola, E. C. van der Linden, D. Anderson, H. McClure, A. Varki and N. M. Varki, *J. Biol. Chem.*, 2003, **278**, 42845–42850.
6 Y. Suzuki, *Biol. Pharm. Bull.*, 2005, **28**, 399–408.
7 R. G. Webster, W. G. Laver, G. M. Air and G. C. Schild, *Nature*, 1982, **296**, 115–121.
8 S. J. Gamblin, L. F. Haire, R. J. Russell, D. J. Stevens, B. Xiao, Y. Ha, N. Vasisht, D. A. Steinhauer, R. S. Daniels, A. Elliot, D. C. Wiley and J. J. Shekel, *Science*, 2004, **303**, 1838–1842.
9 G. N. Rogers, J. C. Paulson, R. S. Daniels, J. J. Shekel, I. A. Wilson and D. C. Wiley, *Nature*, 1983, **304**, 76–78.
10 N. K. Sauter, M. D. Bednarski, B. A. Wurzburg, J. E. Hanson, G. M. Shekel and D. C. Wiley, *Biochemistry*, 1989, **28**, 8388–8396.
11 S. C. Baos, D. B. Phillips, L. Wildling, T. J. McMaster and M. Berry, *Biophys. J.*, 2012, **102**, 176–184.
12 W. J. Lees, A. Spaltenstein, J. E. Kingery-Wood and G. M. Whitesides, *J. Med. Chem.*, 1994, **37**, 3419–3433.
13 W. Weis, J. H. Brown, S. Cusack, J. C. Paulson, J. J. Shekel and D. C. Wiley, *Nature*, 1988, **333**, 426–431.
14 T. K. Dam and F. C. Brewer, *Glycobiology*, 2010, **20**, 1061–1064.
15 N. Horan, L. Yan, H. Isobe, G. M. Whitesides and D. Kahne, *Proc. Natl. Acad. Sci. U. S. A.*, 1999, **96**, 11782–11786.
16 E. W. Adams, D. M. Ratner, H. R. Bokesch, J. B. McMahon, B. R. O'Keefe and P. H. Seeberger, *Chem. Biol.*, 2004, **11**, 875–881.
17 O. Bohorov, H. Andersson-Sand, J. Hoffman and O. Blixt, *Glycobiology*, 2006, **16**, 21C–27C.
18 A. R. Prudden, Z. S. Chinoy, M. A. Wolfert and G. J. Boons, *Chem. Commun.*, 2014, **50**, 7132–7135.
19 J. Stevens, O. Blixt, J. C. Paulson and I. A. Wilson, *Nat. Rev. Microbiol.*, 2006, **4**, 857–864.
20 X. Song, H. Yu, X. Chen, Y. Lasanajak, M. M. Tappert, G. M. Air, V. K. Tiwari, H. Cao, H. A. Chokhawala, H. Zheng, R. D. Cummings and D. F. Smith, *J. Biol. Chem.*, 2011, **286**, 31610–31622.
21 O. Blixt, S. Head, T. Mondala, C. Scanlan, M. E. Huflejt, R. Alvarez, M. C. Bryan, F. Fazio, D. Calarese, J. Stevens, N. Razi, D. J. Stevens, J. J. Skehel, I. van Die, D. R. Burton, I. A. Wilson, R. Cummings, N. Bovin, C. H. Wong and J. C. Paulson, *Proc. Natl. Acad. Sci. U. S. A.*, 2004, **101**, 17033–17038.
22 L. Deng, X. Chen and A. Varki, *Biopolymers*, 2013, **99**, 650–665.
23 R. A. Childs, A. S. Palma, S. Wharton, T. Matrosovich, Y. Liu, W. Chai, M. A. Campanero-Rhodes, Y. Zhang, M. Eickmann, M. Kiso, A. Hay, M. Matrosovich and T. Feizi, *Nat. Biotechnol.*, 2009, **27**, 797–799.
24 L. Wang, R. D. Cummings, D. F. Smith, M. Huflejt, C. T. Campbell, J. D. Gildersleeve, J. Q. Gerlach, M. Kilcoyne, L. Joshi, S. Sema, N.-C. Reichardt, N. P. Pera, R. Pieters, W. S. Eng and L. K. Mahal, *Glycobiology*, 2014, **24**, 507–517.
25 S. Park, J. C. Gildersleeve, O. Blixt and I. Shin, *Chem. Soc. Rev.*, 2013, **42**, 4310–4326.
26 O. Oyelaran, Q. Li, D. Farnsworth and J. C. Gildersleeve, *J. Proteome Res.*, 2009, **8**, 3529–3538.
27 X. Zhou, C. Turchi and D. Wang, *J. Proteome Res.*, 2009, **8**, 5031–5040.
28 K. Godula, D. Rabuka, K. T. Nam and C. R. Bertozzi, *Angew. Chem., Int. Ed.*, 2009, **48**, 4973–4976.
29 S. N. Narla and X.-L. Sun, *Biomacromolecules*, 2012, **13**, 1675–1682.
30 K. Godula and C. Bertozzi, *J. Am. Chem. Soc.*, 2012, **134**, 15732–15742.
31 N. V. Bovin, *Glycoconjugate J.*, 1998, **15**, 431–436.
32 L. M. Chen, O. Blixt, J. Stevens, A. S. Lipatov, C. T. Davis, B. E. Collins, N. J. Cox, J. C. Paulson and R. O. Donis, *Virology*, 2012, **422**, 105–113.
33 S.-K. Choi, M. Mammen and G. M. Whitesides, *J. Am. Chem. Soc.*, 1997, **119**, 4103–4111.
34 M. L. Huang, R. A. A. Smith, G. W. Trieger and K. Godula, *J. Am. Chem. Soc.*, 2014, **136**, 10565–10568.
35 F. Peri, P. Dumy and M. Mutter, *Tetrahedron*, 1998, **54**, 12269–12278.
36 J. Chiefari, Y. K. Chong, F. Ercole, J. Krstina, J. Jeffery, T. P. T. Le, R. T. A. Mayadunne, G. F. Meijs, C. L. Moad, G. Moad, E. Rizzardo and S. H. Thang, *Macromolecules*, 1998, **31**, 5559–5562.
37 J. C. Jewett and C. R. Bertozzi, *Chem. Soc. Rev.*, 2010, **39**, 1272–1279.
38 C. Geisler and D. L. Jarvis, *Glycobiology*, 2011, **21**, 988–993.
39 N. Shibuya, I. J. Goldstein, W. F. Broekaert, M. Nsimba-Lubaki, B. Peeters and W. J. Peumans, *J. Biol. Chem.*, 1987, **262**, 1596–1601.
40 I. Koerner, M. N. Matrosovich, O. Haller, P. Staeheli and G. Kochs, *J. Gen. Virol.*, 2012, **93**, 970–979.
41 Y. Suzuki, Y. Nagao, H. Kato, T. Suzuki, M. Matsumoto and J. Murayama, *Biochim. Biophys. Acta*, 1987, **903**, 417–424.

Electronic Supplementary Material (ESI) for ChemComm.

Electronic Supplementary Information

Determination of receptor specificities for whole influenza viruses using multivalent glycan arrays

Mia L. Huang,[a] Miriam Cohen,[b] Christopher J. Fisher,[a] Robert J. Schooley,[c] Pascal Gagneux , [b] Kamil Godula[a*]

[a] Department of Chemistry and Biochemistry, University of California San Diego, 9500 Gilman Drive, La Jolla, CA 92093. [b] Department of Pathology, Division of Comparative Pathology and medicine, University of California San Diego, 9500 Gilman Drive, San Diego, CA, 92093-0687. [c] Division of Infectious Diseases, Department of Medicine, University of California San Diego, 9500 Gilman Drive, San Diego, CA, 92093-0358.

Table of contents

General materials and methods

All chemicals, unless stated otherwise, were purchased from Sigma Aldrich. Purchased starting materials were used as received unless otherwise indicated. 3'-sialyllactose and 6'-sialyllactose were purchased from Carbosynth (San Diego, CA). Anhydrous dioxane was generated via filtration through basic alumina. Polymers were isolated by gel filtration on Sephadex G-25 columns (PD-10, GE Healthcare). Solvent compositions are reported on a volume/volume basis unless otherwise noted.

Instrumentation

Column chromatography was performed on a Biotage Isolaera One automated flash chromatography system. Nuclear magnetic resonance (NMR) spectra were collected on a Bruker 300 MHz NMR spectrometer. Spectra is recorded in D_2O or D_2O solutions at room temperature and are reported in parts per million (ppm) on the δ scale relative to the residual solvent as an internal standard (for ^1H NMR, D_2O = 4.79 ppm). Size exclusion chromatography was performed on a Hitachi Chromaster system equipped with an RI detector and a 5 μm, mixed bed, 7.8 mm I.D. x 30 cm TSKgel column (Tosoh Bioscience). Polymers were analyzed using an isocratic method with a flow rate of 0.7 mL/min in DMF (0.2% w/v LiBR, 70°C). UV-Vis experiments were performed using a quartz cuvette (10 mm path length) in a Nanodrop2000c spectrophotometer (ThermoFisher). HRMS (high resolution mass spectrometry) analysis was acquired via an Agilent 6230 ESI-TOFMS in either positive or negative ion mode. Polymer glycan ligation reactions were conducted in a Biorad MyCycler thermocycler (Hercules, CA). Graphs were generated using KaleidaGraph (Reading, PA).

Overall Scheme for Mucin Mimetic Glycopolymer Synthesis[1]

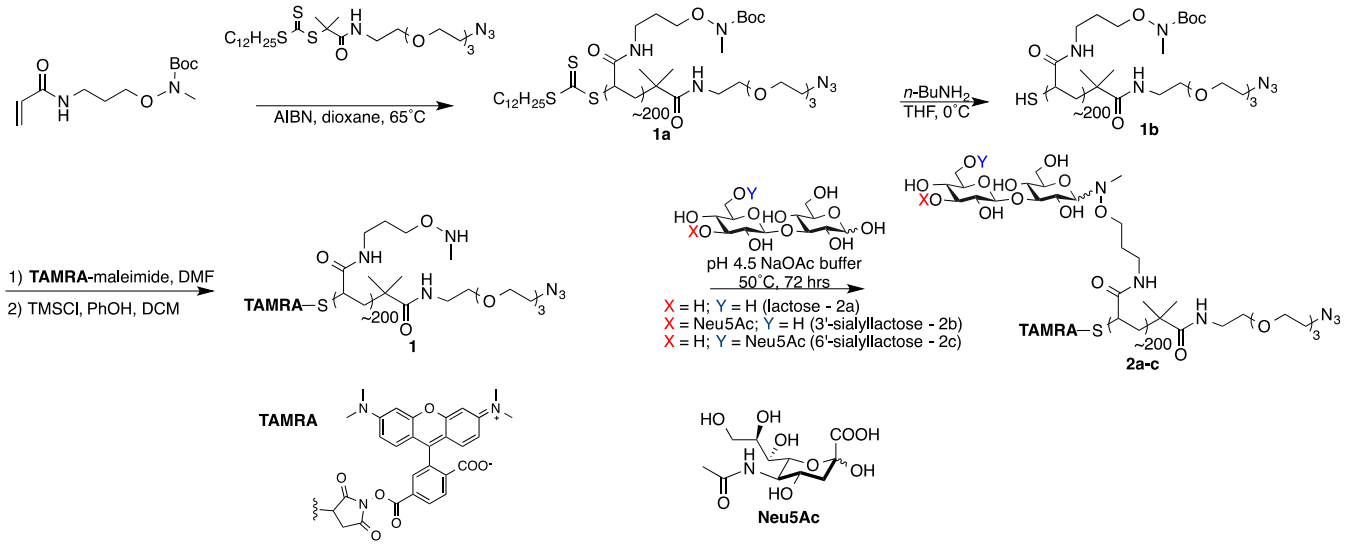

General procedure for RAFT polymerization[2] of *tert*-butyl (3-acrylamidopropoxy)methyl carbamate monomer:

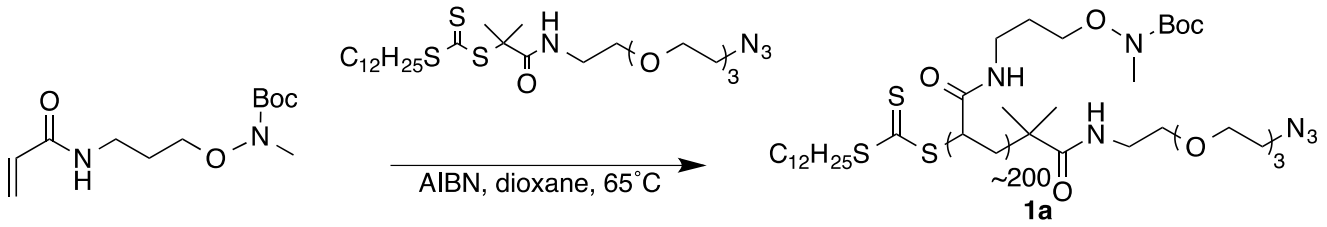

As previously described,[1] a flame-dried Schlenk flask (10 mL) equipped with a magnetic stirring bar was charged with azide chain transfer agent (5.5 mg, 9.74 µmol, 0.33 mol% with respect to *tert*-butyl (3-acrylamidopropoxy)methyl carbamate monomer, AIBN (0.18 mg, 1 µmol, 0.03 mol% with respect to the monomer, delivered as 100 µL of a 10.2 mM solution in anhydrous dioxane, monomer (0.031 mmol AIBN in 3 mL dioxane,), and anhydrous dioxane (650 mg). The flask was equipped with a rubber septum and filled with N_2. The yellow solution was thoroughly degassed by three freeze-pump-thaw cycles. The flask was then allowed to warm to room temperature and then immersed into an oil bath preheated to 65 °C. After 12 hours, the viscous reaction mixture was then diluted in ether and precipitated into excess hexanes with vigorous stirring. The solid residue was then re-dissolved into ether, and precipitated again in hexanes. This precipitation procedure was repeated once more. The faintly yellow polymer was then concentrated from $CHCl_3$ three times to remove residual hexanes and dried under vacuum overnight to yield 1a as a pale yellow solid (518.5 mg, 68.8%). ^{1}H NMR ($CDCl_3$, 300 MHz) δ (ppm): 3.90-3.65 (bs, 2H), 3.35-2.80 (bm, 5H), 1.80-1.05 (bm, 16H). GPC (DMF, 0.2% LiBr): M_w = 55.2 kDa, M_n = 45.7 kDa, DI = 1.18, DP ≈ 200. UV–Vis absorbance at 310 nm ($CHCl_3$, 23 µM) = 0.329.

Figure S1. ^{1}H NMR (300 MHz, $CDCl_3$) of 1a.

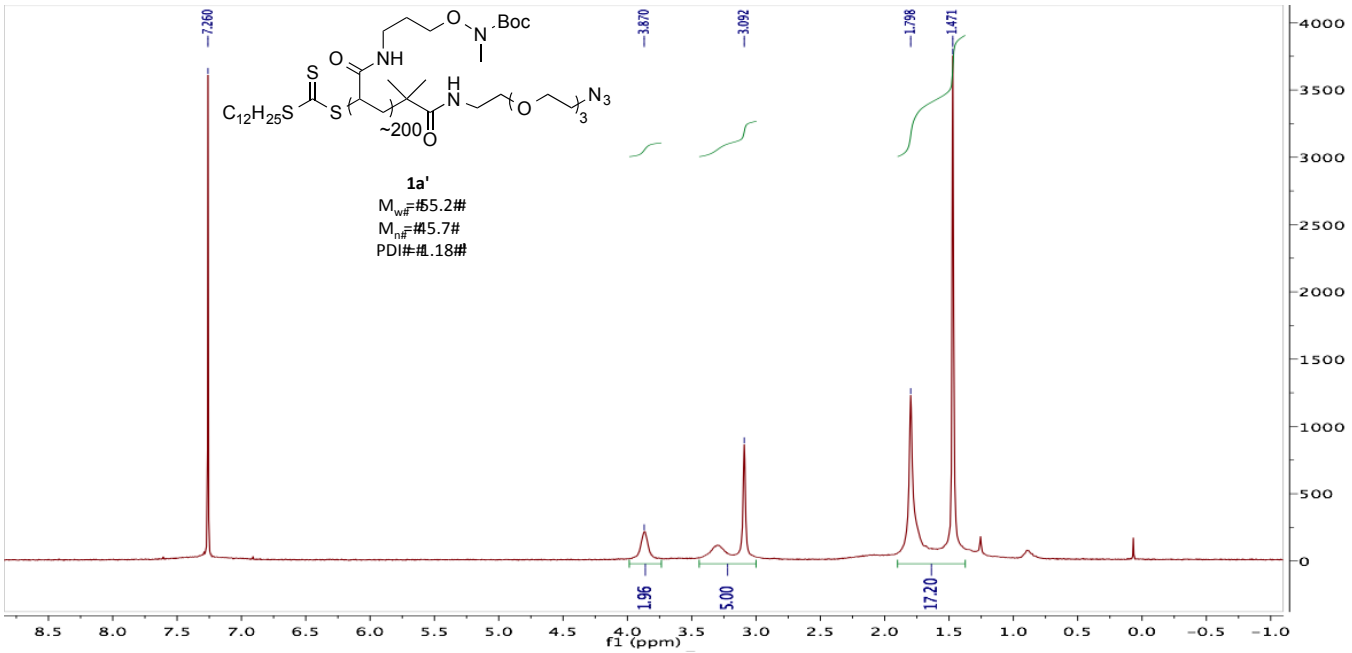

General procedure for the synthesis of end-deprotected polymers:[1]

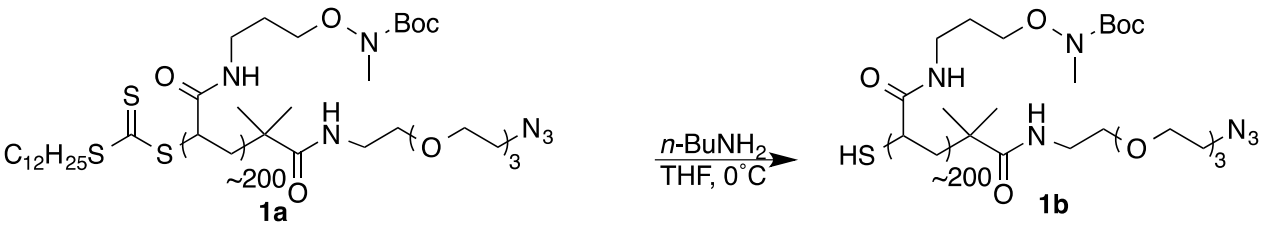

A vial (4 mL) equipped with a magnetic stir bar was charged with 1a (257.21 mg, 2 mM) and 2.30 mL of a degassed 20 mM n-butylamine solution in THF. The vial was submerged in an ice bath and allowed to react for 3.5 hours. The reaction mixture was then diluted in ether and precipitated into excess hexanes with vigorous stirring. The precipitation step was performed three times. The polymer was concentrated from $CHCl_3$ three times to remove residual hexanes and dried under vacuum overnight to give polymer 1b (98.5% yield) as a white solid. ^{1}H NMR ($CDCl_3$, 300 MHz) δ (ppm): 3.87 (bs, 2H), 3.4-3.08 (bm, 5H), 2.13-1.46 (bm, 15H). UV-Vis absorbance at 310 nm ($CHCl_3$, 23 μM) = 0.094.

Figure S2. ^{1}H NMR (300 MHz,$CDCl_3$) 1b.

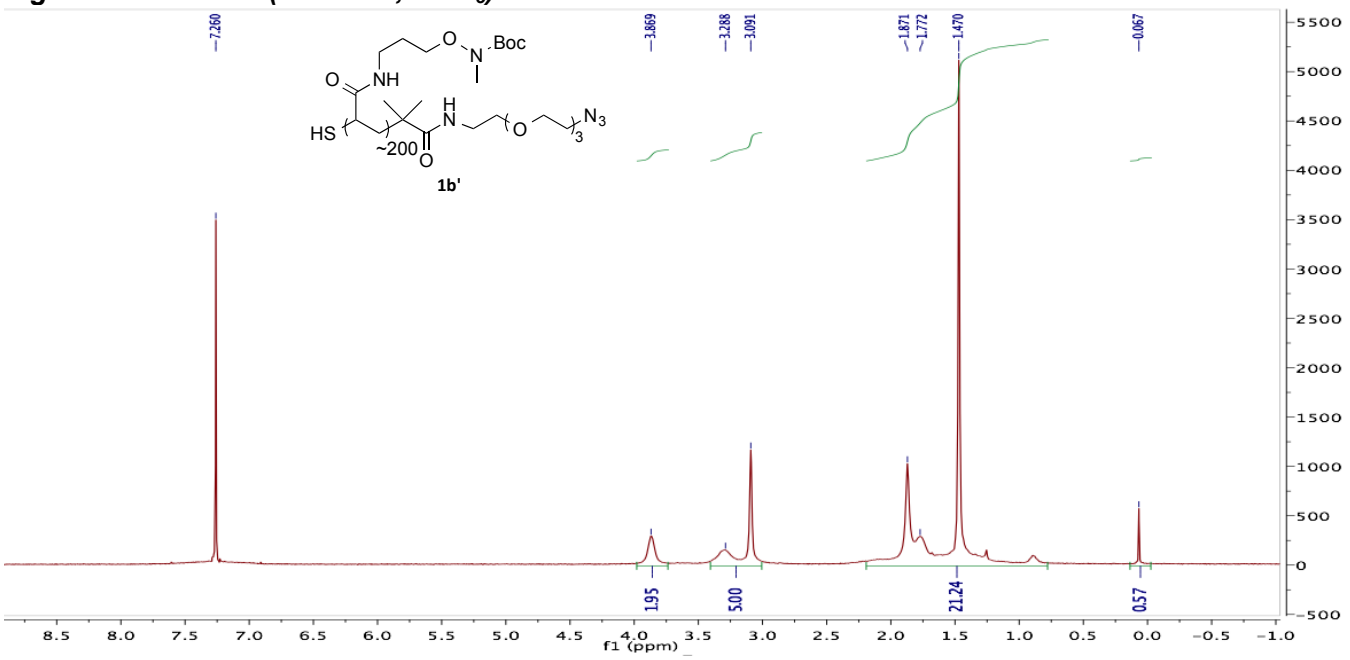

General procedure for the synthesis of fluorophore-labeled polymers and subsequent side chain deprotection:[2]

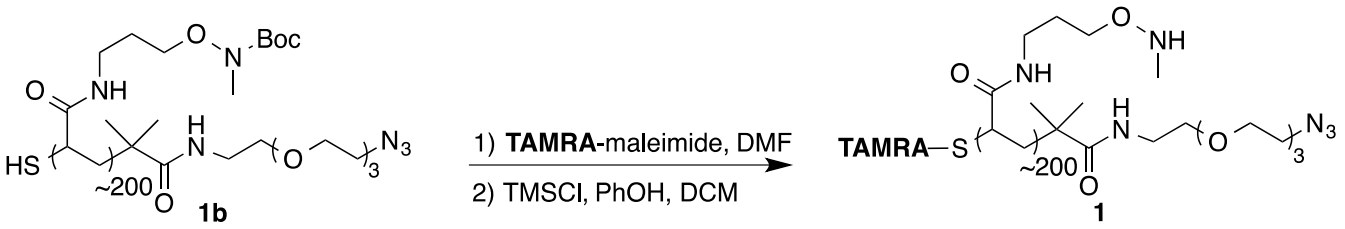

A vial (4 mL) equipped with a magnetic stirring bar, was charged with polymer 1b (45.3 mg) and dissolved in 500 µL of a 2 mM TAMRA C_5-maleimide (1.21 eq) solution in DMF. Following degassing by three freeze-pump-thaw cycles, the reaction mixture was stirred overnight in dark. The reaction mixture was then diluted with ether and precipitated in excess hexanes. The solution was centrifuged (1000 xg, 5 min) and solvent was replaced with fresh hexanes and resubmitted to centrifugation. The precipitation procedure was repeated once more. The polymer was then concentrated from $CHCl_3$ three times to remove residual hexanes and dried under vacuum. Side-chain deprotection was conducted using previously published procedures.[3] To the labeled polymer intermediate, was added 500 □L of a freshly prepared solution of TMS-Cl (1M) and phenol (3M) in anhydrous DCM. The resulting solution was stirred for 2 hours. The polymer is then precipitated by ether and isolated by centrifugation (1000 xg, 3 min), washed 3x with ether, isolated using a PD-10 column, and lyophilized to afford polymer 1. ^{1}H NMR (D_2O, 300 MHz) δ (ppm): 3.71 (bs, 2H) 3.18 (bs, 2H), 2.61 (bs, 3H), 2.1-1.25 (6H, bm). UV-Vis spectrophotometry was used to determine labeling efficiency: (TAMRA, λ_{max}: 556) = 30%.

Figure S3. ^{1}H NMR (300 MHz D_2O) of 1.

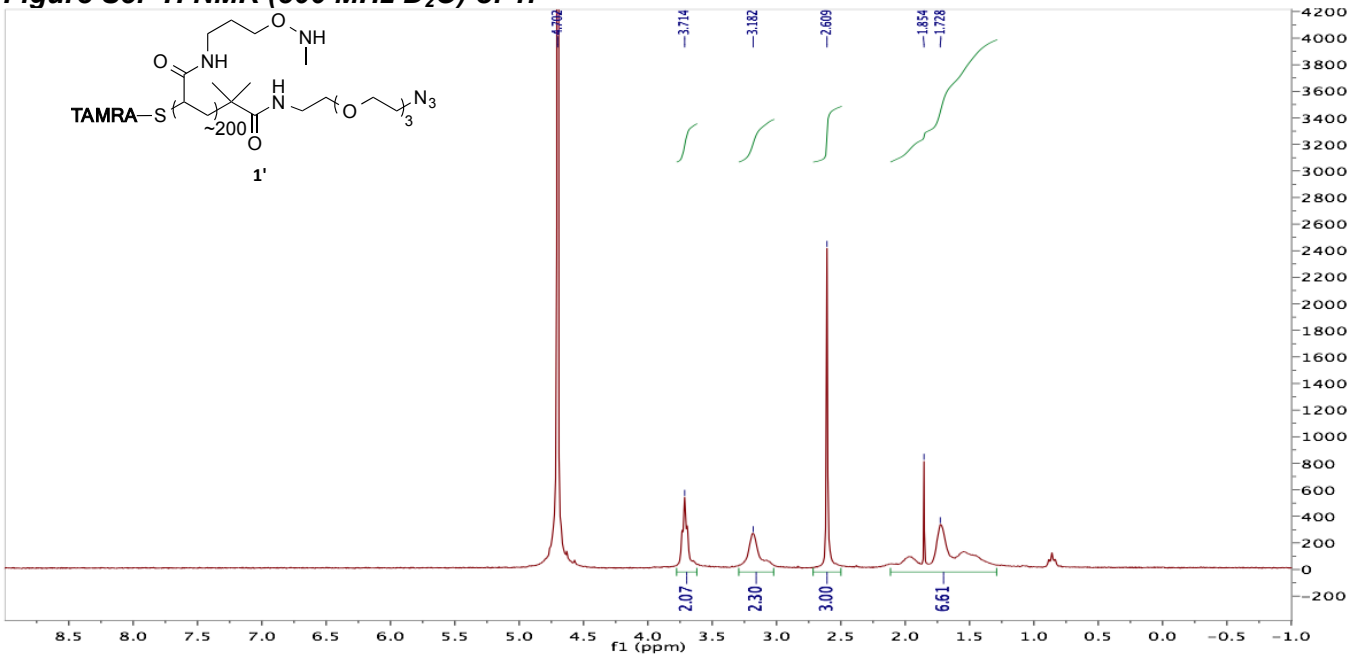

General procedure for glycopolymer synthesis:[1]

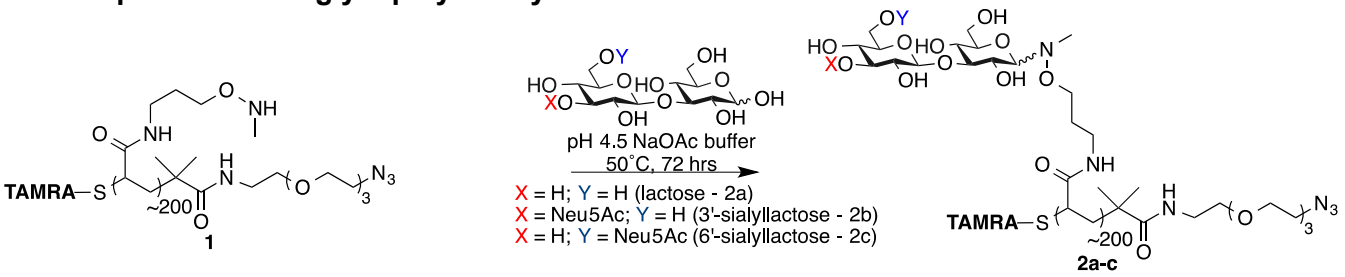

A PCR (0.5 mL) tube containing polymer 1, along with 1.1 eq of glycan was dissolved in sodium acetate buffer (1 M NaOAc, 1 M urea, pH 4.5) to form a 150 mM (by side chain) solution. Following reaction in a thermocycler at 50˚C for 72 hours, the mixture was submitted to an Amicon Ultra Centrifugal Filter (pre-washed with Milli-Q water twice by spin dialysis and overnight incubation in Milli-Q water, 10K MWCO, Millipore), and spin dialyzed (6000 xg, 14 min.) four times using a deuterated phosphate buffered saline solution (100 mM phosphate, 150 mM NaCl, pD 7.4), discarding the flow through and filling to 500 µL each time. Then, the spin column was inverted into a clean centrifuge tube and a solution of 2a-c was collected via centrifugation (1100 xg, 3 min) and analyzed by ^{1}H NMR. Glycan ligation efficiency was determined by subtracting the polymer backbone protons from the total integration in the region □2.5-4.5 ppm relative to the polymer backbone methyl protons (H_a, □□2.4-2.8 ppm), and dividing the difference by the number of glycan protons.

Table S1. Glycopolymer ligation efficiencies (LE) and valences.

Glycopolymer ligation efficiencies were determined by subtracting polymer backbone protons (total of 7 protons) from the total integration in the region δ2.5-4.5 ppm, and dividing the difference by the number of glycan protons. Glycan valency was then calculated as the product of the degree of polymerization and ligation efficiency.

Polymer ID	Glycan	LE (%)	Valency
2a	Lactose	70	140
2b	3' Sialyllactose	45	90
2c	6' Sialyllactose	45	90

Figure S4. ^{1}H NMR spectrum for 2a (300 MHz, deuterated phosphate buffer pD 7.4).

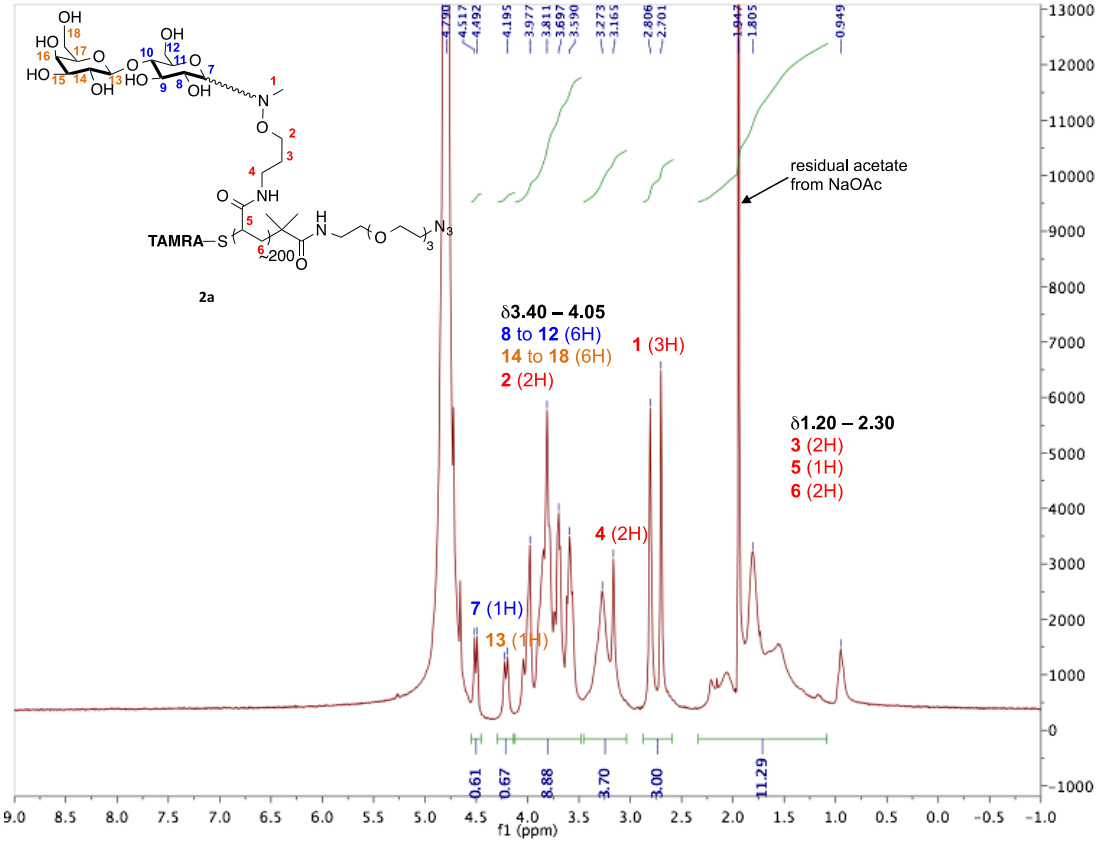

Figure S5. ^{1}H NMR spectrum for 2b (300 MHz, deuterated phosphate buffer pD 7.4).

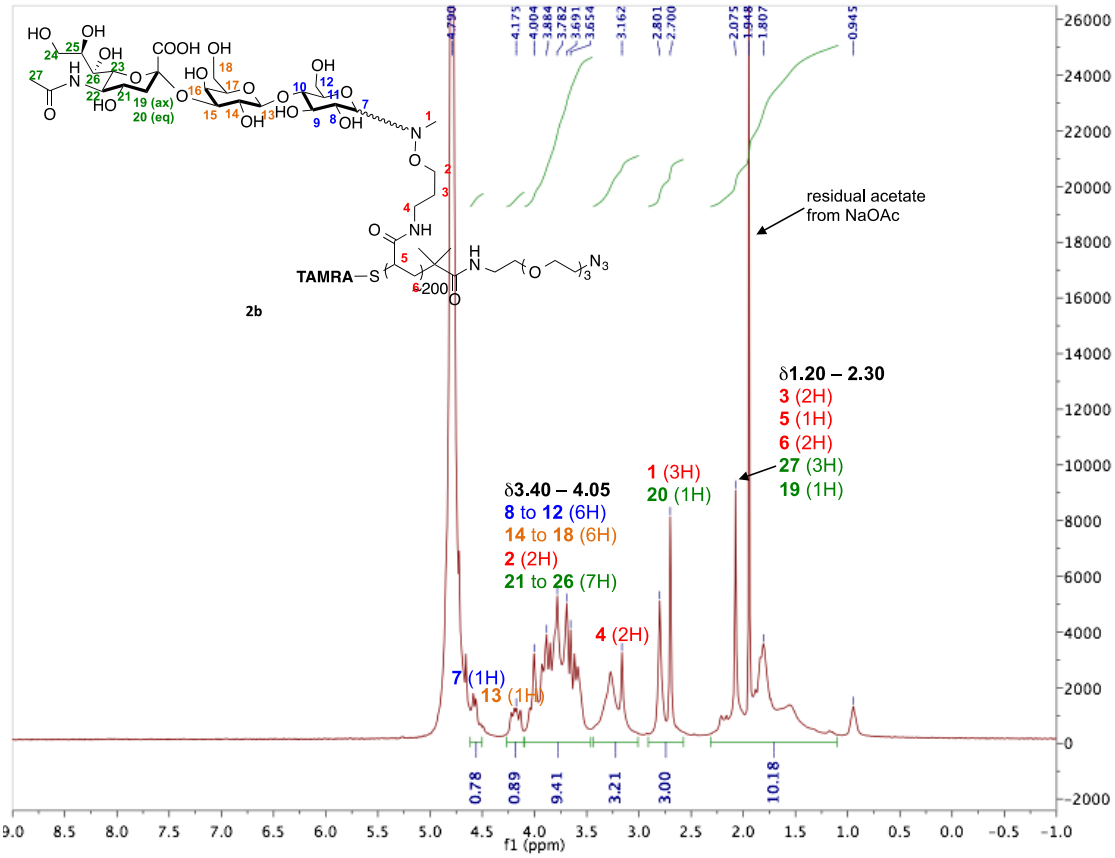

Figure S6. ^{1}H NMR spectrum for 2c (300 MHz, deuterated phosphate buffer pD 7.4).

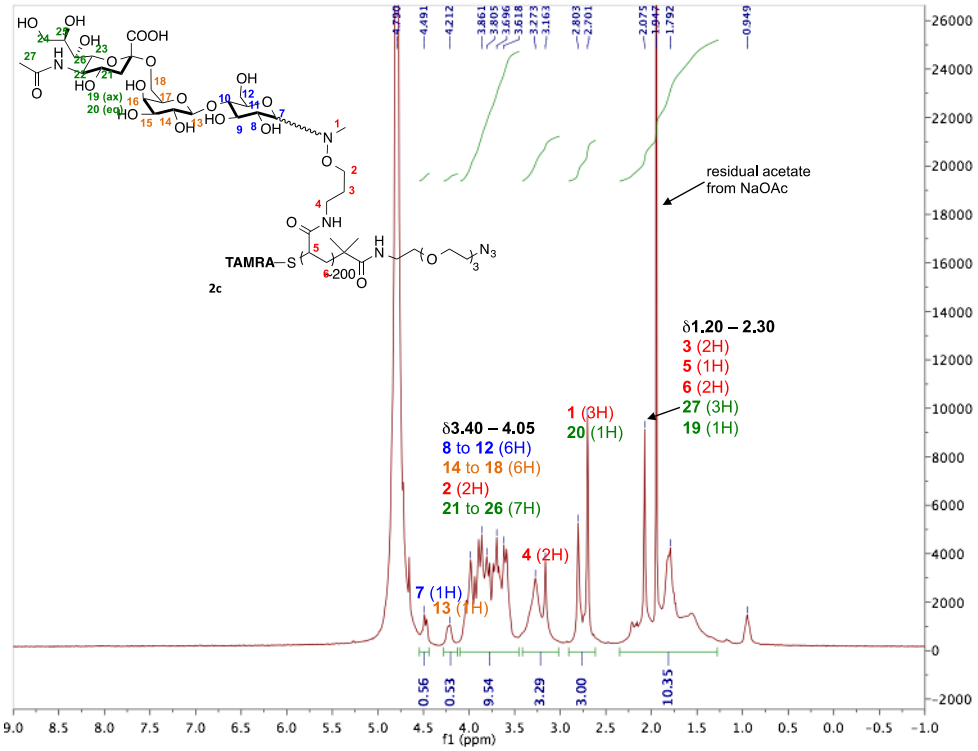

Figure S7. ^{1}H NMR analysis of the hydrolysis of 3'-sialyllactose (500 MHz, 1M deuterated acetic acid, 1 M urea, D_2O, pH 4.5). Minimal hydrolysis of the terminal sialic acid glycosidic bond is observed within 72 hours at 50°C (observed as the appearance of the H3eq proton of free β-Neu5Ac).

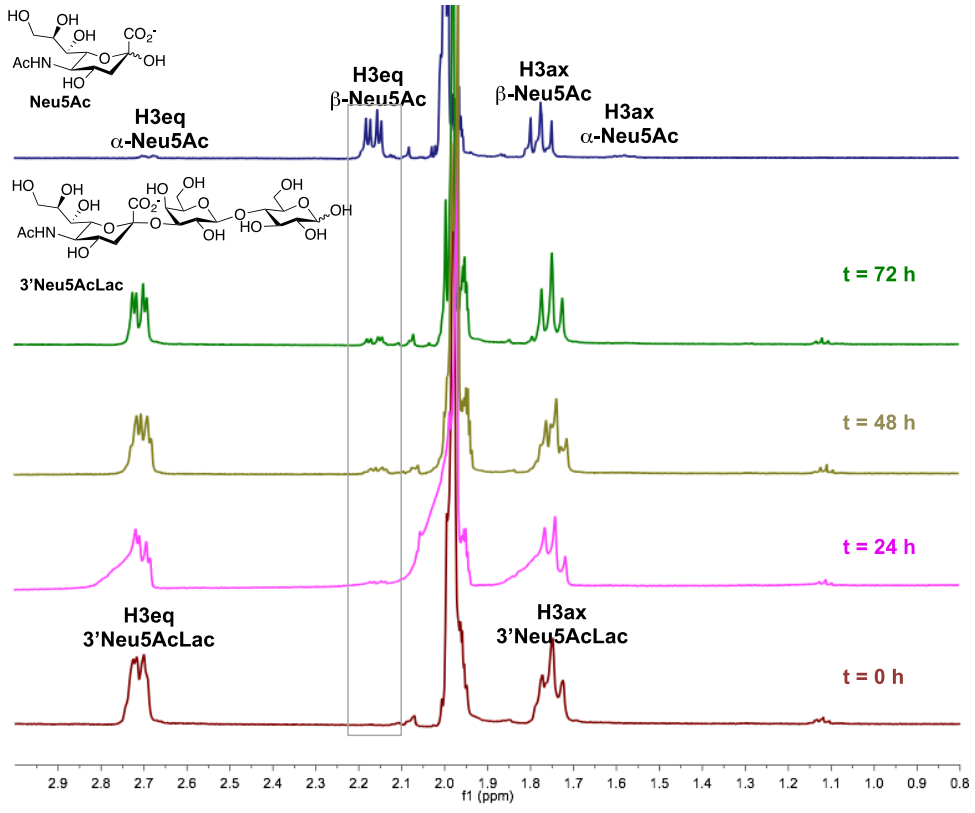

Figure S8. ^{1}H NMR analysis of the hydrolysis of 6'-sialyllactose (500 MHz, 1M deuterated acetic acid, 1 M urea, D_2O, pH 4.5). Minimal hydrolysis of the terminal sialic acid glycosidic bond is observed within 72 hours at 50°C (observed as the appearance of the H3eq proton of free β-Neu5Ac).

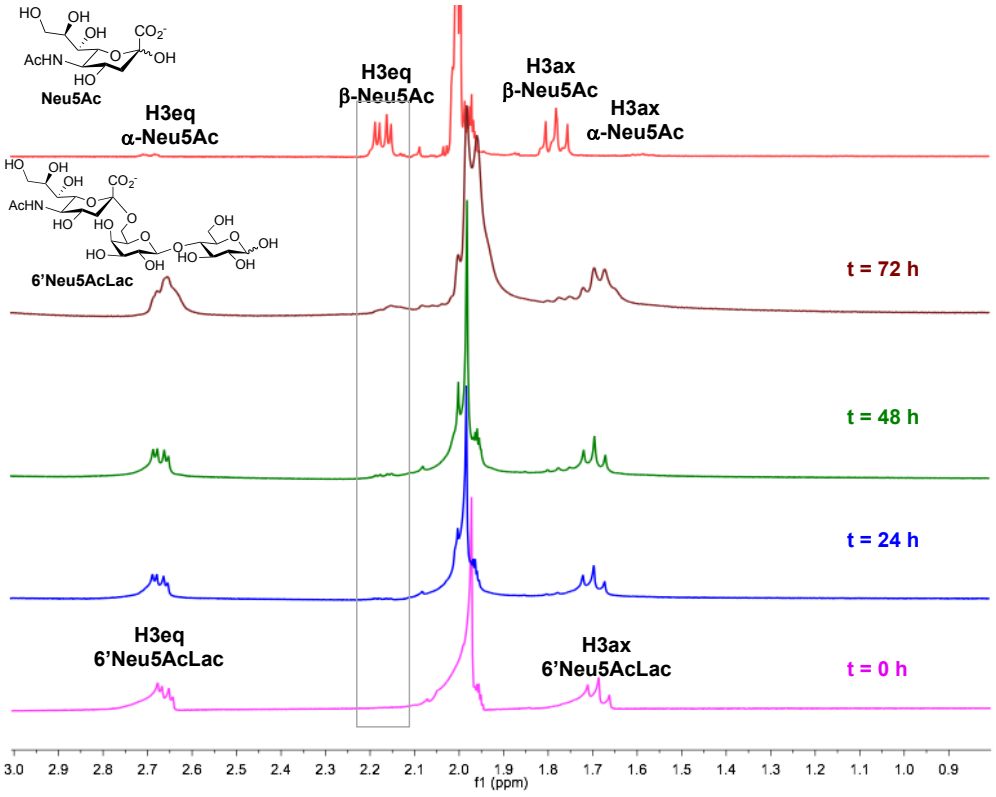

Microarray fabrication

Procedure for generating ADIBO-functionalized slides
To generate azadibenzocyclooctyne (ADIBO)-functionalized slides,[4] the epoxy slides were rinsed with water and allowed to react overnight at room temperature with azadibenzocyclooctyne-amine (1 mM in DMF, 10 mM DIPEA)[5] in a Coplin jar. The slides were then sonicated in methanol (2 x 15 min), rinsed with water, and centrifuged at 500 rpm for 5 min to "spin-dry," and stored at 4°C until use. Prior to printing, the slides were passivated with 1% BSA, 0.1% Tween20 for 1 hr at room temperature, washed with PBS (2 x 15 min), rinsed with water, and spin dried.

Determination of Glycan Concentration for Microarray Printing: Using the TAMRA labeling efficiency (30%), a polymer molarity can be calculated using the dye concentration determined by UV-Vis absorbance at 556 nm. Being that valency represents a ratio of glycans ligated per molecule of polymer, it can be used to stoichiometrically compare moles of glycan to moles of polymer.

[glycan] = [polymer] x (% ligation efficiency)
= [TAMRA] / 0.30 x (% ligation efficiency)

For polymer **2a**, [TAMRA] = 21.5 μM; hence,
[polymer] = 21.5 μM / 0.30 = 71.7 μM, and
[lactose] = 71.7 μM x 70 = 5.0 mM

Procedure for microarray printing
Microarrays were fabricated on epoxide-coated glass (SuperChip, ThermoFisher) using a GIX Microplotter Desktop (Sonoplot, Middleton, WI) and analyzed using a Axon GenePix 4000B microarray scanner (Molecular Devices). For microarray experiments, all water used was doubly-distilled from a Milli-Q water purification system (Millipore). PBS solutions were prepared from a 20X PBS pH 7.5 stock solution (Amresco), filtered through a 0.22 μm membrane filter, and titrated to the desired pH.

The glycopolymers were printed at various concentrations (10 μM – 10 mM, by glycan) on the ADIBO-coated slides at 80-85% relative humidity (in 0.005% Tween, pH 7.4). Each concentration was spotted as four replicate spots, and each slide contained 16 full sub-arrays. To improve spot morphology after printing, the slides were briefly humidified over a 80 deg C water bath and snap-dried over a dry 80 deg C glass surface. The printed slides were allowed to react overnight at 4 deg C. Following a quick rinse with water, the slides were plunged in 0.1% Triton-X/PBS for 2 min, followed by additional 15 min. to remove unbound polymers, washed in PBS (2 x 15 min.), rinsed with water, and spin dried. To create individual sub-arrays on the slide, hydrophobic boundaries were drawn (Invitrogen PAP pen) around each sub-array.

Microarray hybridization with lectins
Biotinylated *Sambucus Nigra* agglutinin (bSNA, Vector labs), biotinylated *Ricinus Communis* Agglutinin I (bRCA, Vector labs), and DyLight649-conjugated *Maackia Amurensis Lectin* (EY Labs) were diluted to 10 nM or 100 nM in PBS / 0.9 mM calcium / 0.4 mM magnesium / 0.02 mM manganese. Arrays were blocked in 1% BSA/PBS for 20 min, rinsed with PBS, incubated with lectins for 1 h at room temperature, and fixed for 15 min with 2% paraformaldehyde in PBS. Slides were washed with PBS/ 0.05% Tween-20, lectin binding was detected by incubating with streptavidin-conjugated Cy5 (Invitrogen) for 30 min.

Figure S9. Microarrayed glycopolymers (**1**, **2a-c**) scanned at 535 nm (TAMRA fluorescence, green) and 635 nm (Cy5 fluorescence, red) following incubation with biotinylated lectins (**A**) RCA120, (**B**) SNA and subsequent staining with Cy5-streptavidin, or fluorophore-conjugated lectin (**C**) Dylight649-MAA. (**D**) Negative control experiments (no lectin) indicate minimal background fluorescence (647, 535: 500, 260 PMT)

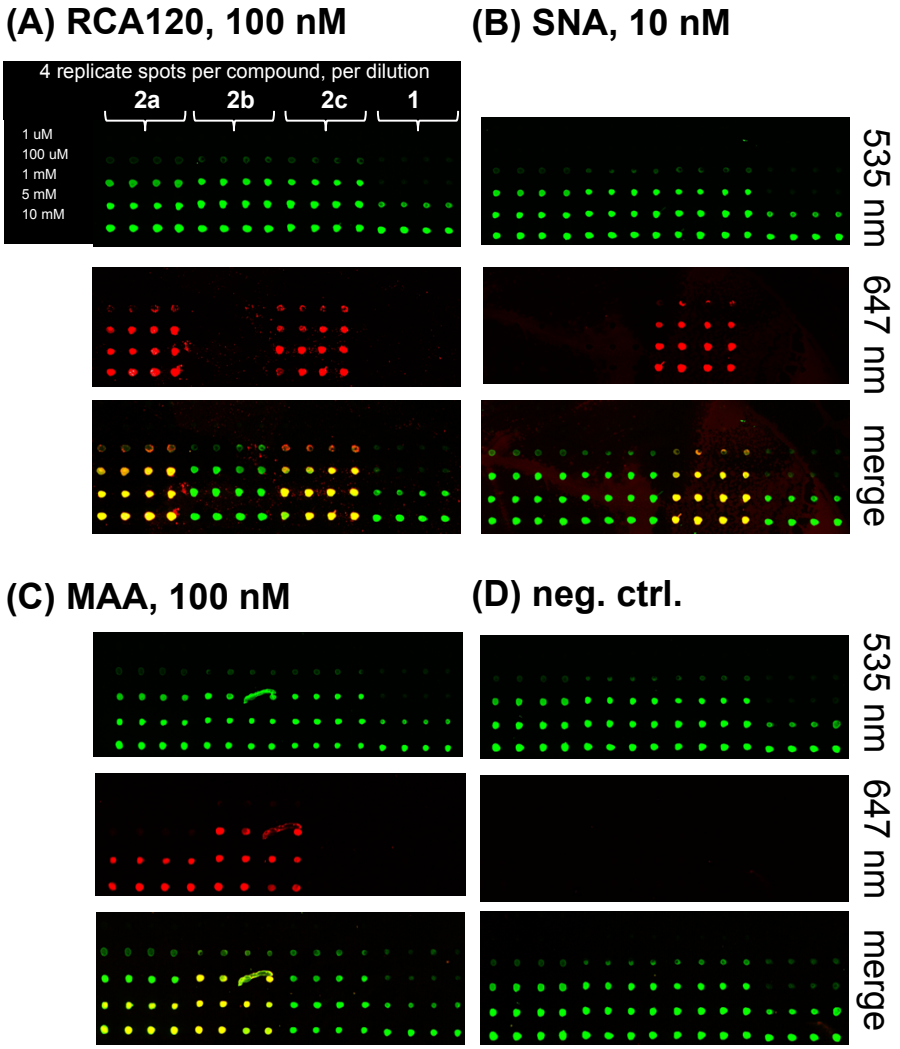

Results. Although RCA120 (*Ricinus communis* agglutinin 120) is generally known as a galactose-specific plant lectin, its binding site accommodates changes in the 6'-galactose position but not in the 3' position. Thus, in addition to lactose, galactose derivatives substituted at the 6'-position (e.g. sialyllactose) have been shown to bind to RCA120, whereas 3'-sialyllactose does not.[6]

Virus production

Two influenza strains A/PR/8/34(H1N1) and A/Aichi/2/68(H3N2) were purchased from ATCC. MDCK cells (ATCC CCL-34) were maintained in Dulbeco's modified Eagle's medium (DMEM, Cellgro) supplemented with 10% fetal calf serum (FCS). All viruses were propagated in MDCK cells that were transferred to DMEM medium supplemented with 0.2% BSA fraction V (EMD), 25mM HEPES buffer (Gibco), 2 μg/ml TPCK-trypsin (Worthington Corporation), and 1% penicillin/streptomycin.

Incubation of microarrays with viruses

The arrays were blocked with 1% BSA/PBS (20 min, RT), and rinsed with PBS. Virus binding to the array was evaluated by incubating A/PR/8/34 (H1N1) at ~1000 or ~500 HAU (hemagglutinating units), or A/Aichi/2/68(H3N2) at the same HAU for 1 hr at RT. Viral stocks were concentrated using a Microcon-50 filtration system (Millipore) when necessary. Viruses were diluted in PBS (0.9 mM calcium, 0.4 mM magnesium) to the appropriate HAU concentration. Following incubation with the viruses, the slides were washed extensively in PBS and fixed with 2% para-formaldehyde in PBS for 15 min. Viral binding was detected by incubation with anti-H1 (A/California/06/09, IA-01SW-0100, eEnzyme) or anti-H3 (A/Shandong/9/99, MIA-H3-246, eEnzyme) antibodies for 30 min, followed by goat-anti-rabbit-IgG-Alexa647 (A31573, Invitrogen) or goat-anti-mouse-IgG-Cy5 (A10523, Invitrogen) antibodies, respectively. Antibodies were diluted in 1% BSA/PBS/0.05% Tween20, and washed post fixation in PBS/0.05%Tween20.

Figure S10. Microarrayed glycopolymers (**1**, **2a-c**) were scanned at 535 nm (TAMRA fluorescence, green) and 647 nm (Cy5 fluorescence, red) following incubation with whole viruses H1N1 (**A** and **B**) or H3N2 (**D** and **E**) at various HAU (hemaglutinnation units) and immunostaining with Cy5-labeled antibodies. (**C** and **F**) Negative control experiments (no virus) indicate minimal background fluorescence from anti-H1 and anti-H3 antibodies, respectively. (647nm, 535nm: 600, 260 PMT).

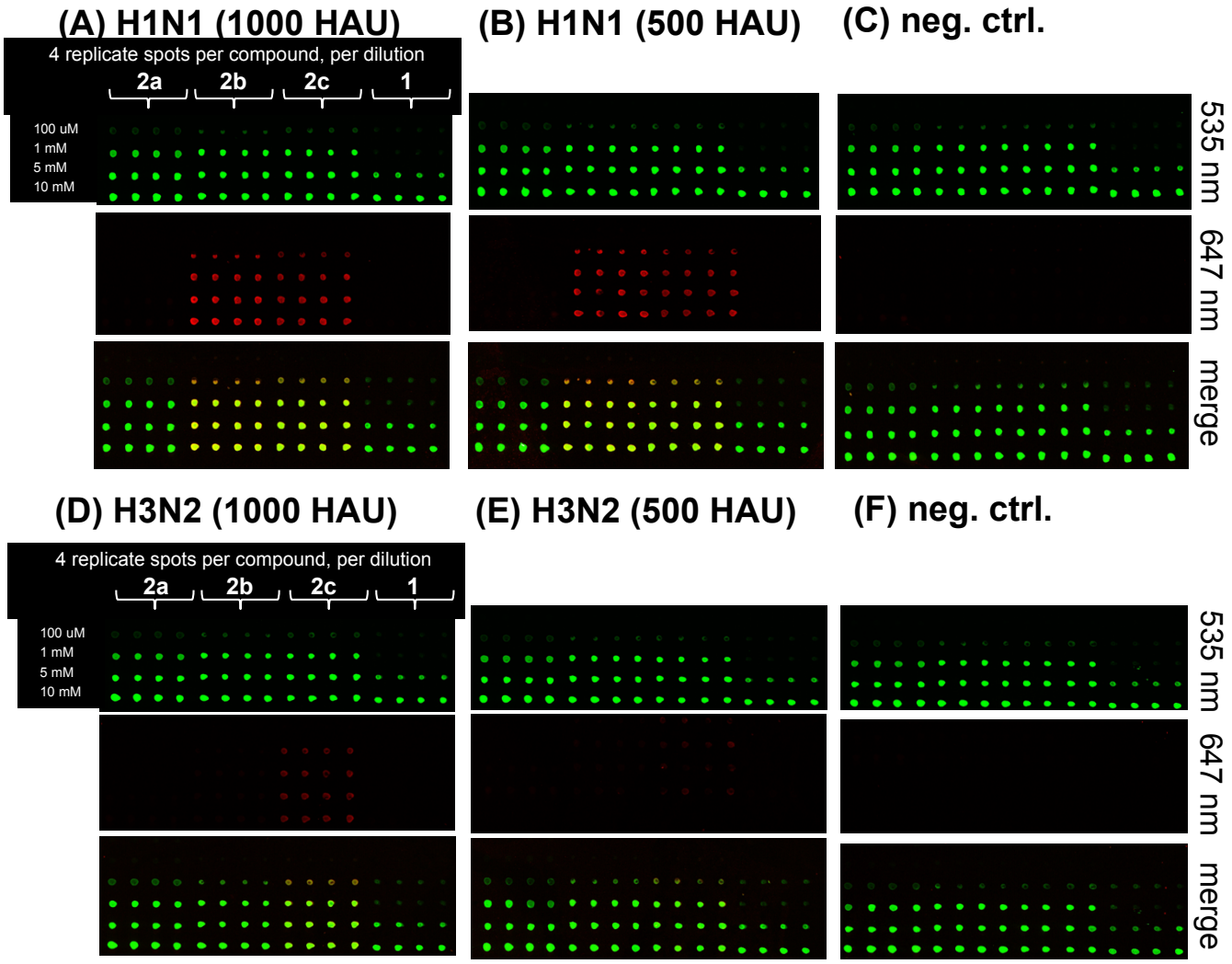

Figure S11. Microarrayed glycopolymers (**1**, **2a-c**) were scanned at 535 nm (TAMRA fluorescence, green) and 647 nm (Cy5 fluorescence, red) following incubation with whole H1N1 viruses at 64 HAU and immunostaining with Cy5-labeled antibodies. (647nm, 535nm: 800, 300 PMT).

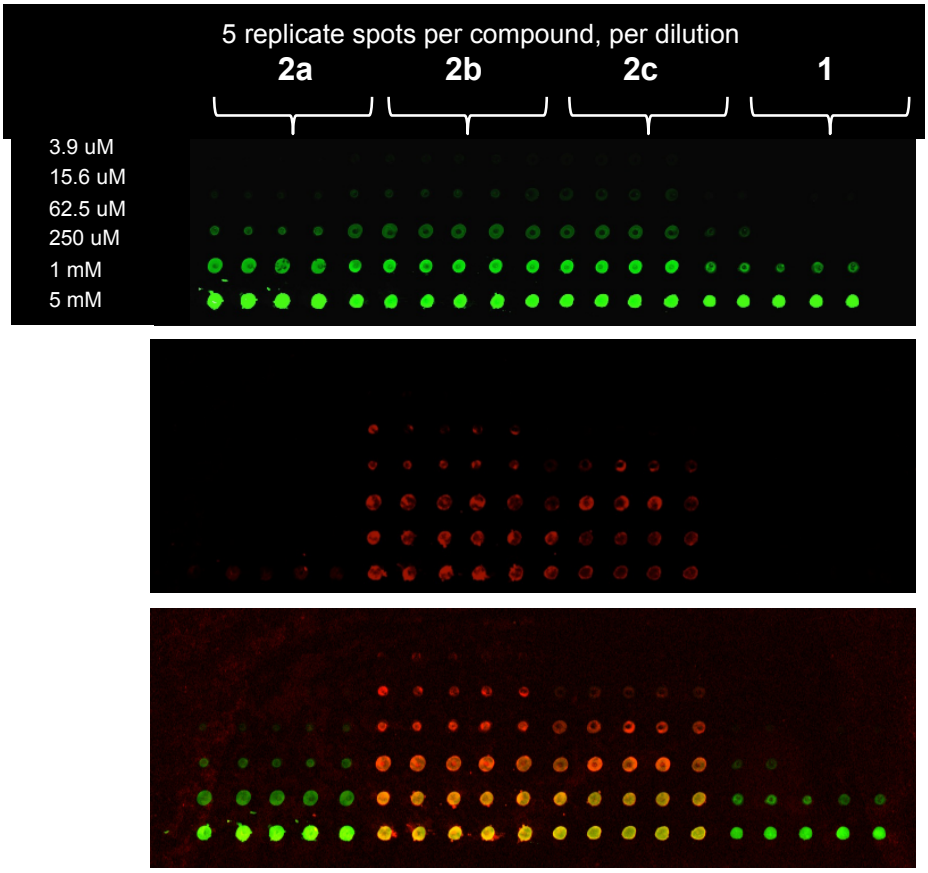

REFERENCES:

1 M. L. Huang, R. A. A. Smith, G. W. Trieger, K. Godula. *J. Am. Chem. Soc*., 2014, **136**, 10565-10568.

2 J. Chiefari, Y. K. Chong, F. Ercole, J. Krstina, J. Jeffery, T.P.T. Le, R.T. A. Mayadunne, G. F. Meijs, C.L. Moad, G. Moad, E. Rizzardo, S.H. Thang, *Macromolecules* 1998, **31**, 5559-5562

3 E. Kaiser, F. Picart, T. Kubiak, J.P. Tam, R. B. J. Merrifield, *Org. Chem.*, 1993, **58**, 5167-5175**.**

4 A. Kuzmin, A. Poloukhtine, M. A. Wolfert, V. V. Popik, *Bioconj. Chem.* 2010, **21**, 2076-2085.

5 X. Ning, J. Guo, W. M. Wolfert, G. J. Boons. *Angew. Chem., Int. Ed. Engl.* 2008, **47**, 2553-2555.

6 M. Fais, R. Karamanska, S. Allman, S. A. Fairhurst, P. Innocenti, A. J. Fairbanks, T. J. Donohoe, B. G. Davis, D. A. Russell, R. A. Field. *Chem. Sci.* 2011, **2**, 1952-1959.